OAK RIDGE
NATIONAL LABORATORY
MANAGED BY UT-BATTELLE
FOR THE DEPARTMENT OF ENERGY

ORNL/NRC/LTR-03/03

ANALYSIS OF A MELCOR INPUT DECK FOR THE PEACH BOTTOM ATOMIC POWER STATION

Robert L. Sanders

OAK RIDGE NATIONAL LABORATORY LIBRARIES
3 4456 0536874 0

UT-BATTELLE
ORNL-27 (4-00)

This report was prepared as an account of work sponsored by an agency of the United States Government. Neither the United States Government nor any agency thereof, nor any of their employees, makes any warranty, express or implied, or assumes any legal liability or responsibility for the accuracy, completeness, or usefulness of any information, apparatus, product, or process disclosed, or represents that its use would not infringe privately owned rights. Reference herein to any specific commercial product, process, or service by trade name, trademark, manufacturer, or otherwise, does not necessarily constitute or imply its endorsement, recommendation, or favoring by the United States Government or any agency thereof. The views and opinions of authors expressed herein do not necessarily state or reflect those of the United States Government or any agency thereof.

ORNL/NRC/LTR-03/03

ANALYSIS OF A MELCOR INPUT DECK FOR THE PEACH BOTTOM ATOMIC POWER STATION

Robert Sanders

February 2003

Prepared by
OAK RIDGE NATIONAL LABORATORY
P.O. Box 2008
Oak Ridge, Tennessee 37831-8057
managed by
UT-Battelle, LLC
for the
U.S. DEPARTMENT OF ENERGY
under contract DE-AC05-00OR22725

CONTENTS

Page

CONTENTS iii

LIST OF FIGURES v

ACRONYMS vii

ANALYSIS OF A MELCOR INPUT DECK FOR THE PEACH BOTTOM ATOMIC POWER STATION 1

INTRODUCTION 1

BACKGROUND 1

METHODOLOGY OF REVIEW 2

REVIEW 2

HS Package 2

CAV Package 2

RN (Radionuclide) Package 2

CF (Control Function) Package 2

CVH/FL (Control Volume Hydrodynamics/Flow Path) Package 2

COR Package 3

CONCLUSION 7

LIST OF FIGURES

Page

Figure 1. Detail of the temperature profile of the innermost radial ring for the bottommost axial level. 8

Figure 2. Temperature profile of lower-head penetrations and two innermost lower head nodes. 9

Figure 3. Comparison of penetration temperature in the inner radial ring as the water level drops. 10

Figure 4. Mass ejection from the lower plenum to the drywell. 11

Figure 5. Temperature profile of debris in lower head. 12

ACRONYMS

ac	alternating current
ADS	automatic depressurization system
BH	Bottom Head
BNL	Brookhaven National Laboratory
BWR	boiling water reactor
CAV	Cavity
CF	Control Function
COR	Core
CVH/FL	Control Volume Hydrodynamics/Flow Path
dc	direct current
dT/dz	representation of fluid temperature profile vs axial height
H	hydrogen
HS	Heat Structure
ICS	isolation cooling system
K	kelvin
kg	kilogram
LOCA	loss-of-coolant accident
m	meter
MELCOR	Name of computer code
MSIV	main steam isolation valves
ORNL	Oak Ridge National Laboratory
PCCS	passive containment cooling system
PWR	pressurized water reactor
RCIC	reactor core isolation cooling
RN	Radionuclide
s	second
SBGTS	StandBy Gas Treatment System
SBWR	simplified boiling water reactor
SNL	Sandia National Laboratories
W	watt

ANALYSIS OF A MELCOR INPUT DECK FOR THE PEACH BOTTOM ATOMIC POWER STATION

INTRODUCTION

At the request of the Sandia National Laboratories (SNL), a review has been completed of a MELCOR input deck for the Peach Bottom Atomic Power Station that models a majority (if not all) of the emergency core cooling systems. Also modeled is the containment spray function of the residual heat removal systems as well as the leakage path amongst the various reactor-building floors. Included in the deck is a vast array of control functions that mimic the automatic and some of the manual operations that are performed after a reactor trip signal occurs. Intrinsic to these control functions is the ability to operate valves and pumps automatically at the required set points without the user having to stop and restart the code to change either a valve position or to start a pump. This provides a great advantage to the user in performing "what if" calculations. The user need only worry about establishing the initial conditions, i.e., failure of a valve or pump, and the input deck should mimic standard plant operation to recover from this imposed variant.

The MELCOR input deck was provided by Mark Leonard of dycoda, LLC, who programmed the large array of control functions that mimic not only the operation of the safety systems but also the manual operation of the safety relief valves for proper temperature control in the wet well. The intent of the input deck appears to be aiding in the development of accident mitigation schemes for the U.S. Nuclear Regulatory Commission. By modeling the safety systems, the user can play "what if" scenarios according to what equipment or regions of the plant are damaged by an external force.

BACKGROUND

The input deck is based on the original input deck utilized by Juan Carbajo of the Oak Ridge National Laboratory (ORNL) in the preparation of the report "Severe Accident Source Term Characteristics for Selected Peach Bottom Sequences Predicted by the MELCOR Code," NUREG/CR-5942. Carbajo produced the input deck based on a deck that was received from Brookhaven National Laboratory (BNL). The BNL input deck was written for MELCOR Version 1.8.0. He modified the deck to utilize the enhancements provided in MELCOR 1.8.1 KH.

The input deck reviewed was written for MELCOR 1.8.5 RF. Thus, significant modifications had to be included. One such change was to the designation of the stainless steel components, which includes the description of the core plate. In previous versions of the code, a simple designation was made as to the function of the stainless steel components. In the current version, special designation of the function of the varied types of steel components in a cell can be provided to the code, e.g., supportive versus non supportive. In addition to updating the deck, other significant modifications and improvements have been made. One such modification is to provide additional volumes in the drywell as well as in the core region. The additional volumes in the core region were required to aid the dT/dz model. In addition, these volumes enhance the flow model within the core by allowing for more representative modeling of flow blockages by debris as well as cross flows once the channel boxes fail. Also in the core region, the first two radial rings were divided in half, making a total of 5 radial rings. Correspondingly, additions were made to the Heat Structure (HS) Package to model these additional volumes in the reactor building. The input to the Cavity (CAV) Package was also enhanced to model the pedestal region more precisely.

METHODOLOGY OF REVIEW

The review consisted of an overview of the input deck as a whole rather than checking the accuracy of the specific input values utilized in the deck. The information reviewed was the sensible operation of the safety systems via the control functions. The input parameters for the COR (Core) Package were reviewed in greater detail because of their impact on melt progression.

To test the model, a short-term station blackout analysis was run that simulates the calculation performed by Carbajo. For this calculation, the short-term station blackout input deck was modified to include dc (direct current) power, but only for 6 hours. In addition, reactor core isolation cooling (RCIC) was modified to force its dependency on ac (alternating current) power alone. Thus, the input deck was modified to a short-term station blackout with the automatic depressurization system (ADS) operational.

REVIEW

The following is a summary of the evaluation of the input deck along with the results of the short-term station blackout. The comments are divided according to the respective MELCOR Package where they apply:

HS Package

Based on the casual overview of the input deck, no recommendations or major deficiencies were found.

CAV Package

Based on the casual overview of the input deck, no recommendations or major deficiencies were found.

RN (Radionuclide) Package

Based on the casual overview of the input deck, no recommendations or major deficiencies were found.

CF (Control Function) Package

The following are two recommendations for changes to the input values used in the control set input portion of the deck:

The specified available life of the battery should be reduced to 6 hours. From discussions with ORNL's Steve Hodge, 8 hours may be an overestimate of the operational life. If 8 hours are to be used, a proper reference should be obtained from the BWR Owners Group.

Since the terry turbine associated with the RCIC system has a significant probability of failure, the ability to allow for ADS without RCIC operation is highly desirable.

CVH/FL (Control Volume Hydrodynamics/Flow Path) Package

No significant problems were found within these packages. However, the following are some recommendations that should be included in the model:

1. A path should be added from a recirculation line to the drywell to simulate a LOCA (loss-of-coolant accident) within the drywell.
2. The model should include a control function to warn the user if containment sprays cause a vacuum within the drywell.
3. The arbitrary volume of the steam turbine for RCIC may be too small, causing a Courant-limit problem. This is based on experience with modeling the isolation cooling system (ICS) and passive containment cooling system (PCCS) associated with the Simplified Boiling Water Reactor (SBWR). However, a direct effect on the time step from the RCIC turbine volume was not noted in the test calculations performed.
4. Leakage through the main steam isolation valves (MSIVs) should be considered for inclusion in the model. This would also involve creation of the vacuum line from the condenser to the environment. It should be noted that the overall effect of this path would be small, based on the fission product plate-out that would occur in the steam lines and the condenser.
5. The StandBy Gas Treatment System (SBGTS) is not modeled. From discussions with Randy Gauntt of Sandia, this was not an oversight but a planned omission based on the conclusion that the SBGTS would not be available after an accident. Verification with plant personnel should be established and documented to support this conclusion.
6. A path should be added to model the ability to provide water injection to the reactor vessel via the bottom-head drain line.
7. Lastly, the description of the model provided specifies that the core spray injection is connected to the lower head CVH volume, but the input provided has the injection going into Volume CV350.

COR Package

The input to the COR Package is by far the most important and critical in determining melt progression and mitigation. In examining the input for the COR Package, several philosophical differences between work performed at Oak Ridge versus Sandia were discovered. The first and most important is the absence of the Bottom Head (BH) Package. It is believed by Oak Ridge that the BH Package is a much more mature technique to handle the way in which debris is modeled in the lower plenum versus those contained in the COR Package. The benefits of the BH Package will be discussed later. As stated earlier, the input deck, specifically the COR Package input deck, is based largely on the original MELCOR input, which was created by BNL for Version 1.8.0. The input has been modified to utilize the latest features in the code, but the basic design data utilized remains from the original deck. Of particular significance is the lack of incorporation of the new fuel design. The fuel design utilized in the input deck is based on the older 8x8 fuel assembly and not the current higher pin-number design. The newer design also utilizes partial length fuel rods, which can be easily modeled within the COR Package. Additional information can be provided to Sandia on the new fuel design, if required.

The following are comments on several input parameters for the COR Package input:

1. The radiation view factor on card COR00003 from the liquid pool to core components was decreased dramatically from 0.95 to 0.25 in the current input deck. Better justification needs to be provided for this significant reduction.
2. The fission power control function specified on card COR0004 determines the fission power based on the water level in the downcomer region. Thus, the distribution of fission power Control Function number should be greater than 100 to allow fission power to be distributed only over liquid-covered cells containing intact fuel.

3. The refreezing heat transfer coefficients are significantly higher than the default values. Better justification should be provided.

4. On card COR00009, a penetration failure temperature of 1870 K is used. This value seems very high. From my test calculations, this leads to a significant late penetration failure. Also, penetration failure (which includes guide-tube and instrument-tube failure within the lower plenum) is based on temperatures in the first axial level, which is typically the crust layer and is cooler. Some latitude should be allowed to represent higher temperatures in axial levels between the core plate and the second axial level, the region containing the middle of the debris bed; the majority of the decay heat would exist in this middle layer, leading to high temperatures. At these temperatures, the guide tubes and instrument tubes would melt, allowing melt ejection to occur sooner than currently predicted. This will be discussed in more detail later.

   The BH Package contains algorithms that represent the failure of guide and instrument tubes within the debris bed.

5. Of significant importance is the input on COR00012, which controls the parameters in the falling debris quench model. In the input deck provided by Sandia, the heat transfer coefficient from in-vessel falling debris to the pool is given as 220.0 W/m^2-K. The input deck states that this value is based on the median value of "SNL H2 PWR study." However, in a boiling water reactor (BWR), significant interferences exist in the lower plenum (the guide tubes) that do not exist in a PWR (pressurized water reactor); therefore, falling debris would tend to be held up and break apart, resulting in a lower fall velocity and greater "effective" heat transfer. Thus it is highly recommended that the heat transfer coefficient be increased and the fall velocity decreased.

   It is important to note that all the debris is believed to be quenched during the fall process before striking the bottom head. Therefore, our guidelines have been to use values that produce the expected end result and not worry so much about the intermediate state, i.e., the instantaneous heat transfer is not important as long as the proper end-state is achieved with the proper energy balance.

6. For the debris porosity given on card CORZjj01, the debris porosity should be increased to ensure lower-plenum dryout. In earlier versions of MELCOR, the hot molten debris would effectively push the water out of the way, attack the lower head, and fail a penetration, forcing vessel ejection immediately following initial core-plate failure.

7. In card CORRZZ05, both the channel and bypass flow have been changed. No justification for either was provided.

8. Card CORRZZ04, the same value for particulate debris equivalent diameter, should be used in both the core region as well as the lower plenum.

9. On CORPENR, the specified surface area is significantly lower than previously used; better justification should be provided since this appears to be a very important parameter with regard to melt progression.

10. It should be noted that the default COR Package eutectic model is not utilized in this calculation. Given the current state of this model within MELCOR, this is the only viable option. However, to mimic important eutectic interaction within the core region, lower melting temperatures are utilized for key material. From discussions with Randy Cole, it appears that this eutectic representation is appropriate for the core region in which boundaries exist to limit the types of interaction that could occur. However, this may not be appropriate for the lower plenum late in the accident where a conglomeration of the material exists. Again, the BH Package provides a much better representation of eutectic interactions within this hodgepodge of material.

Prior to the discussion of the two major inconsistencies that were found, it is important to note the timing of some of the important events:

1. Initial core-plate failure occurred at 11,683 s in Ring 1 by yielding.
2. Core-plate failure in Ring 2 at 13,264 s by yielding.
3. Column failure in Cell 205 at 13,316 s; also, core-plate structure in Ring 2 can no longer support core.
4. Core-plate failure in Ring 2 for loss of mass at 13,316 s.*
5. Core-plate failure in Ring 3 at 18,710 s by yielding.
6. Column failure in Cell 305 at 19,222 s; associated core-plate structure in Ring 3 can no longer support core.
7. Core-plate failure in Ring 3 for loss of mass at 19,432 s.*
8. Dryout occurs at approximately 21,275 s after scram.
9. Column failure in cells 103, 104, and 105 at 23,535 s; associated core-plate structure in Ring 1 can no longer support core.
10. Column failure in Cell 405 at 24,102 s by yielding, and associated core-plate failure in Ring 4.*
11. Column failure in Cell 204 at 24,192 s.
12. Column failure in cells 303 and 304 at 24,426 s.
13. Column failure in Cell 102 at 24,542 s.
14. Column failure in Cell 203 at 24,647 s.
15. Column failure in cells 403 and 404 at 25,104 s.
16. Column failure in Cell 302 at 25,115 s.
17. Column failure in Cell 202 at 25,293 s.
18. Column failure in Cell 505 at 25,625 s and associated core-plate failure in Ring 5.
19. Core-plate failure in Ring 4 at 25,766 s by yielding.
20. Column failure in Cell 402 at 25,808 s by yielding.
21. Column failure in Cell 301 at 26,396 s by yielding.
22. Column failure in cells 502, 503 and 504 at 26,826 s, yielding
23. Core-plate failure in Cell 405 at 26,851 s by loss of mass.
24. Column failure in Cell 201 at 27,279 s by yielding.
25. Core-plate failure in Ring 1 at 27,697 s, by loss of mass.
26. Core-plate failure in Ring 5 at 28,384 s by yielding.
27. Column failure in Cell 101 at 30,074 s by yielding.
28. Core-plate failure in Ring 5 at 31,265 s, by loss of mass.
29. Column failure in Cell 401 at 36,327 s by yielding.

---

* Indication of core-plate failure in each radial ring.

30. **Lower-head-penetration failure in Ring 1 at 41,303 s start of ejection.**[†]
31. **Lower-head-penetration failure in Ring 2 at 42,234 s.**[†]
32. Column failure in Cell 501 at 43,667 s by yielding.
33. **Lower-head-penetration failure in Ring 3 at 43,672 s.**[†]
34. The majority of material ejection has ended by 45,000 s.
35. Calculation stopped by rupture of Cavity 0 at 82,852 s.

In addition to the above information, it is important to determine the point at which lower-plenum dryout occurs. From Figure 1, dryout occurs slightly after 21,000 s. In NUREG-5942, dryout was reported to occur at approximately 13,000 s. The difference between these values is most likely the result of the initial conditions, an improved core-plate model, and/or smaller radial rings. In NUREG/CR-5942, initial core-plate failure was predicted at slightly before 10,000 s, as opposed to the value given above of nearly 12,000 s. Therefore, core-plate-failure time is not that significantly different. Thus, the largest effect is most likely the reduction in relocating mass as a result of the smaller radial rings.

It is important to remember that when the hot material enters the hot lower plenum, a large amount of steam is produced, cooling the core plate and structures in the other radial rings, i.e., prolonging further core-plate failure and lower-plenum dryout.

Figure 2 shows the temperature profile of the penetrations and the innermost regions of the lower head. As can be seen from the figure, the penetrations heat up gradually after core-plate failure until around 20,000 s when a sharp drop in temperature occurs. Figure 3 provides a greater detail of this drop for the innermost radial ring. The apparent cause of this temperature drop will be discussed later.

Because of this temperature drop, melt ejection is delayed until after 41,000 s, as seen in Figure 4. Again from NUREG/CR-5942, melt ejection was previously determined to occur at slightly after 16,000 s. Examining Figure 5, which shows the debris-bed temperatures starting at 25,000 s, the debris-bed temperatures are in excess of the temperature required to fail the interstitial stainless-steel guide tubes. Therefore, melt ejection should have occurred significantly earlier than predicted; this is the first inconsistency.

Because of the late melt ejection, a large portion of the debris is liquid or extremely hot. This leads to the second questionable result: the speed that material is ejected through the penetration. Starting at 41,303 s (the first penetration failure) to 42,234 s (second penetration failure), material is ejected at a very large rate, nearly 210,000 kg of material is ejected (over half of the total ejected mass) or an average rate of 226 kg/s. As stated, this is a direct result of the delay in failure of the penetrations and the buildup of molten material within the debris bed. Because of this large melt ejection, the vessel itself never fails, and all material exits through the penetrations.

Thus, it is apparent that mass ejection from the vessel is dependent on the failure mechanism of the penetrations alone. Because of this dependence, a thorough examination of the heat-up of the penetrations was performed. During this examination, a discontinuity in the temperature profile of the penetrations was discovered, as noted above and shown in Figure 3. The problem appeared to occur during lower-plenum dryout. When the swollen water level drops to the top of the first axial level, as seen in Figure 3, the temperature of the penetrations drops nearly 500 degrees. This inconsistency is

[†] Indication of penetration failure in each radial ring.

probably related to a change in the models associated with the regime change, i.e., in going from water covered to a mixture of both air and water.

CONCLUSION

From the spot-check review, the input deck represents very well the core injection systems for a Mark-I containment, including both the ac-driven systems as well as the back-up RCIC driven by a terry turbine. Included in the model are flow paths that represent the major drywell-leakage pathways to the environment. For the test calculation performed, the input deck performed well with no critical errors or calculation bombs.

In conclusion , the major deficiency discovered in the input deck was in the choice of lower-head model. The current input utilizes the model inherent in the COR Package. This model in the present version of MELCOR performs better than in previous versions; however, sufficient deficiencies still exist to warrant the examination of using the BH Package. The most important of these is the ability to model guide-tube failure within the "hot" debris bed.

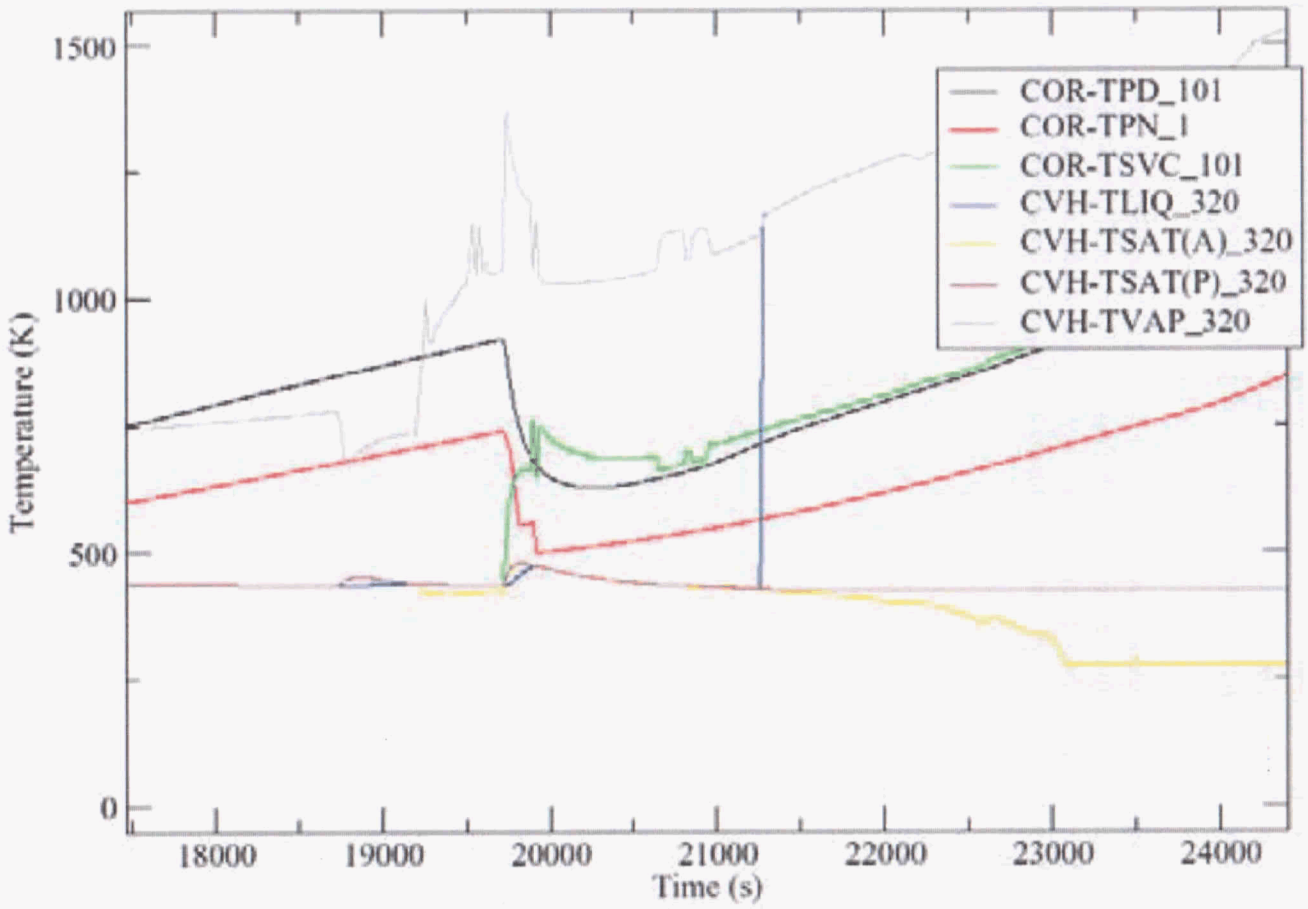

Figure 1. Detail of the temperature profile of the innermost radial ring for the bottommost axial level.

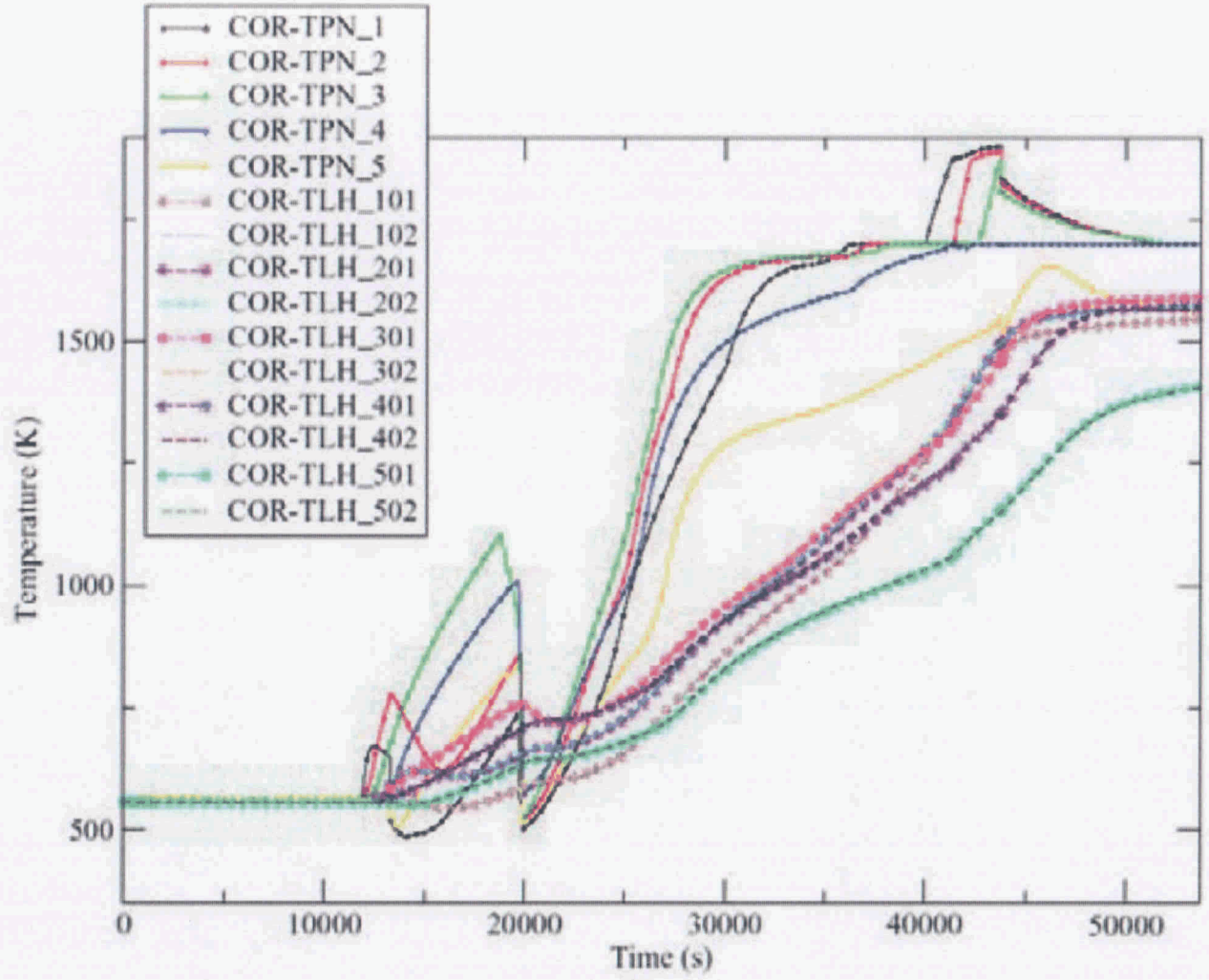

Figure 2. Temperature profile of lower-head penetrations and two innermost lower head nodes.

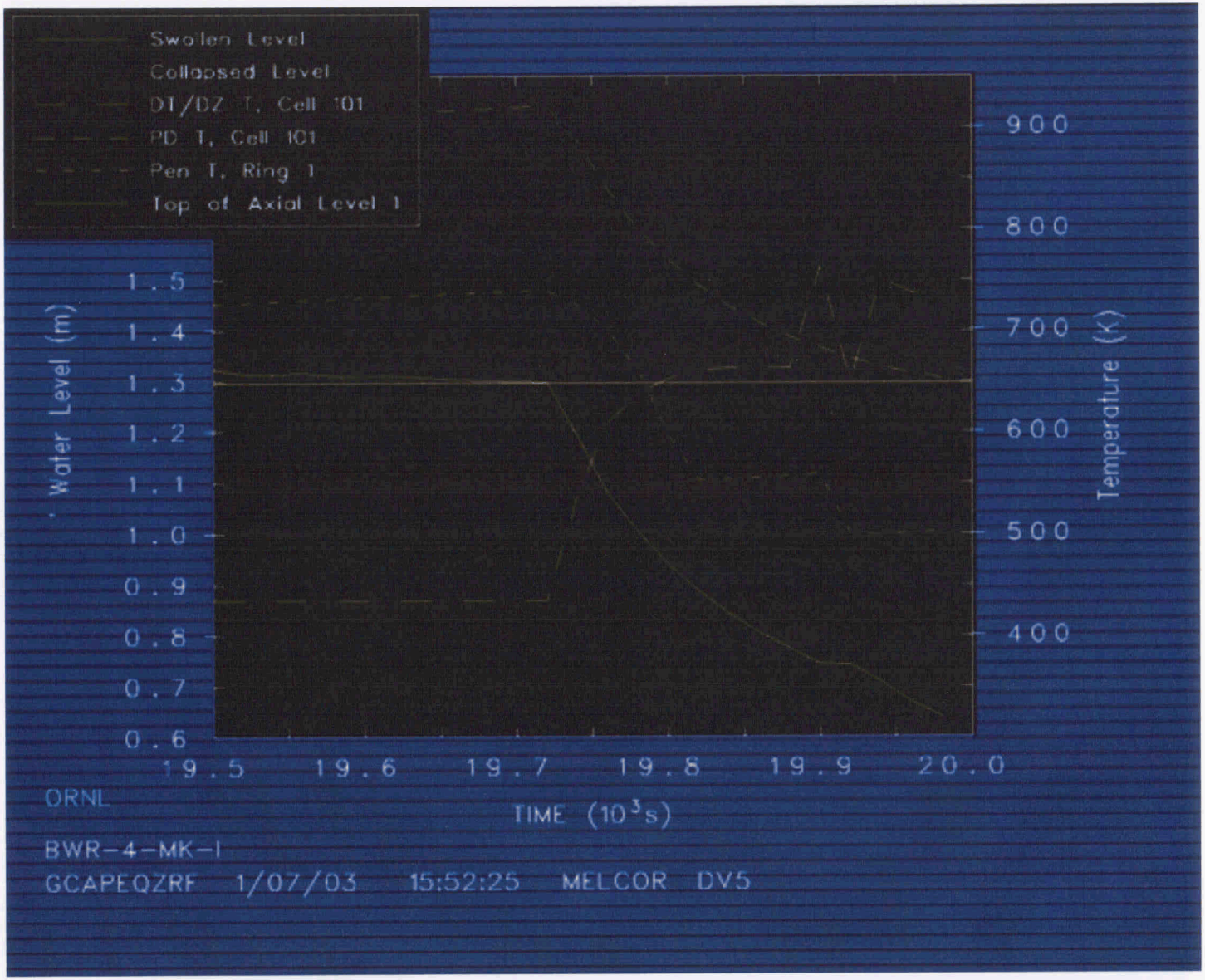

Figure 3. Comparison of penetration temperature in the inner radial ring as the water level drops.

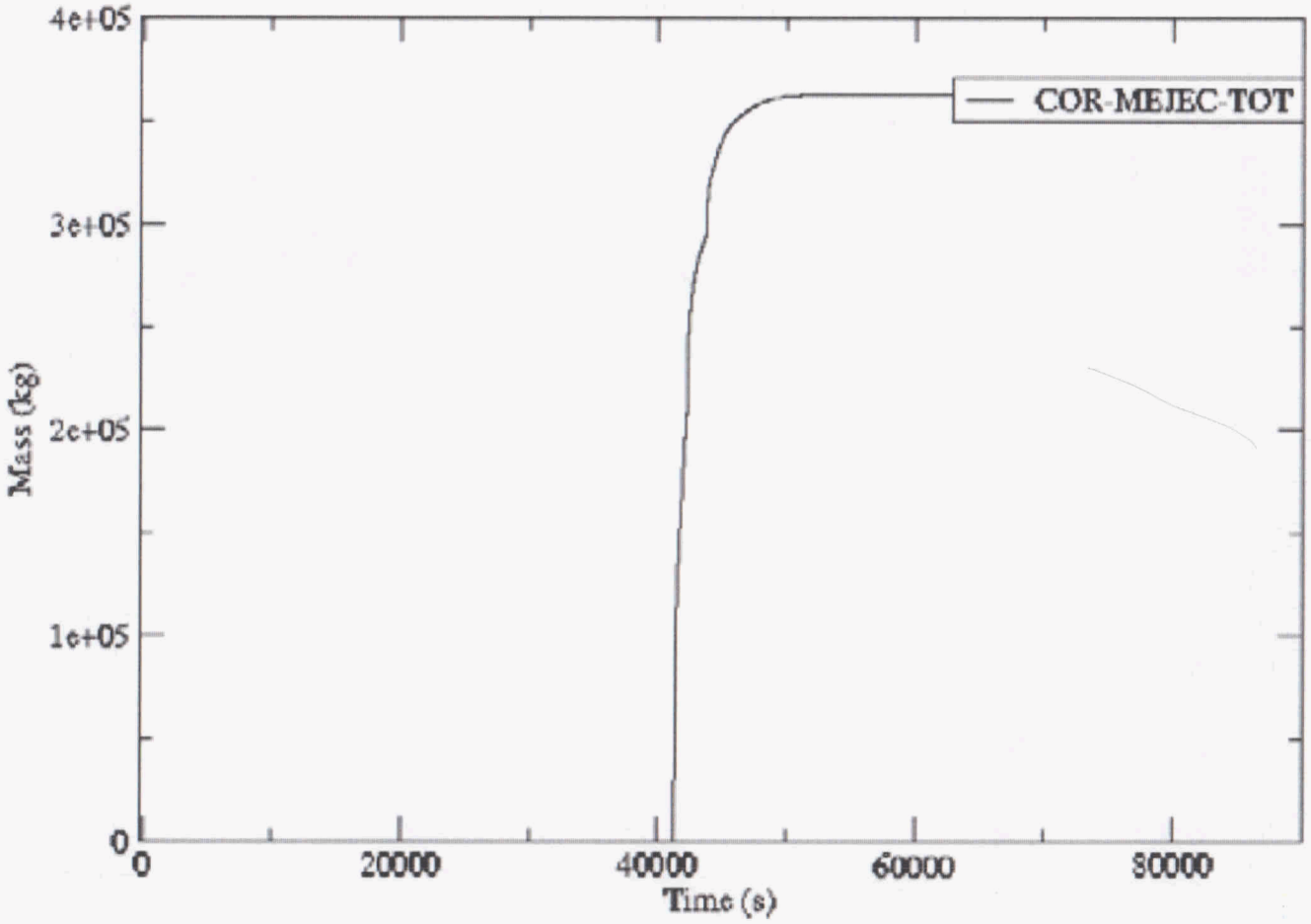

Figure 4. Mass ejection from the lower plenum to the drywell.

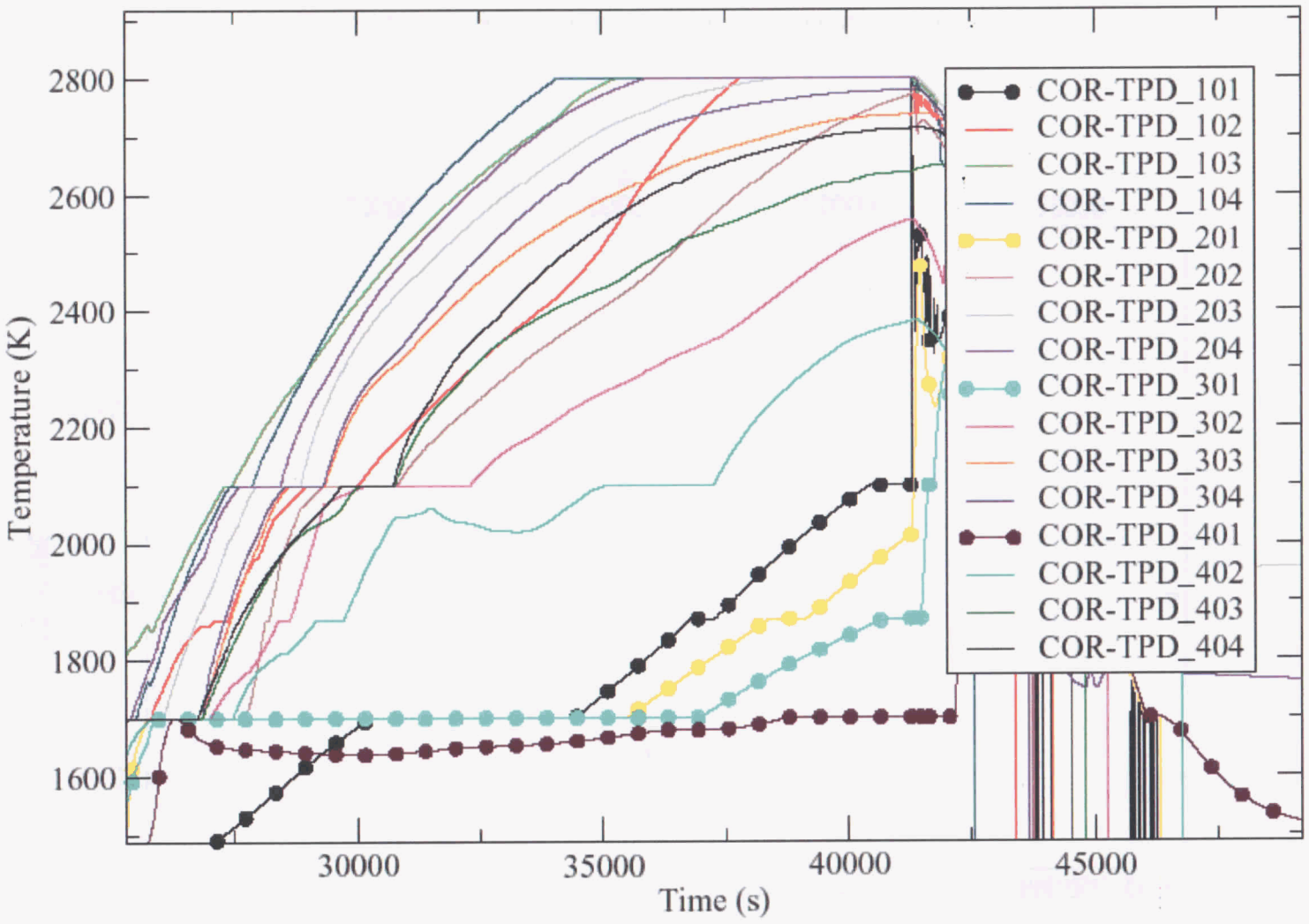

Figure 5. Temperature profile of debris in lower head.

INTERNAL DISTRIBUTION

1. S. A. Hodge
2. R. H. Morris
3. R. L. Sanders
4. C. D. Sulfredge
5. Central Research Library
6. ORNL Laboratory Records-RC
7. ORNL Laboratory Records-OSTI

EXTERNAL DISTRIBUTION

8. Randy Gauntt, Sandia National Laboratories, P.O. Box 5800, Albuquerque, NM 87185-0748
9. Mark Leonard, dycoda, LLC, 70 Andres Sanchez Road, Belen, NM 87002
10. Jason H. Schaperow, U.S. Nuclear Regulatory Commission, Location: TWFN, Bldg. 10F28, Mail Stop: 10K8, Washington, DC 20555-0001
11. Charles G Tinkler, Jr., U.S. Nuclear Regulatory Commission, Location: TWFN, Bldg. 10E31, Mail Stop: 10K8, Washington, DC 20555-0001